

Improved source apportionment of organic aerosols in complex urban air pollution using the multilinear engine (ME-2)

Qiao Zhu¹, Xiao-Feng Huang^{1,*}, Li-Ming Cao¹, Lin-Tong Wei¹, Bin Zhang¹, Ling-Yan He¹, Miriam Elser², Francesco Canonaco², Jay G. Slowik², Carlo Bozzetti², Imad El-Haddad², and André S.H. Prévôt²

¹Key Laboratory for Urban Habitat Environmental Science and Technology, School of Environment and Energy, Peking University Shenzhen Graduate School, Shenzhen, 518055, China.

²Paul Scherrer Institute (PSI), 5232 Villigen-PSI, Switzerland

Abstract Organic aerosols (OAs), which consist of thousands of complex compounds emitted from various sources, constitute one of the major components of fine particulate matter. The traditional positive matrix factorization (PMF) method often apportions aerosol mass spectrometer (AMS) organic datasets into less meaningful or mixed factors, especially in complex urban cases. In this study, an improved source apportionment method using a bilinear model of the multilinear engine (ME-2) was applied to OAs collected during the heavily polluted season from two Chinese megacities located in the north and south with an Aerodyne high-resolution aerosol mass spectrometer (HR-ToF-AMS). We applied a rather novel procedure for utilization of prior information and selecting optimal solutions, which do not necessarily depend on other studies. Ultimately, six reasonable factors were clearly resolved and quantified for both sites by constraining one or more factors: hydrocarbon-like OA (HOA), cooking-related OA (COA), biomass burning OA (BBOA), coal combustion (CCOA), less-oxidized oxygenated OA (LO-OOA) and more-oxidized oxygenated OA (MO-OOA). In comparison, the traditional PMF method could not effectively resolve the appropriate factors, e.g., BBOA and CCOA, in the solutions. Moreover, coal combustion and traffic emissions were determined to be primarily responsible for the concentrations of PAHs and BC, respectively, through the regression analyses of the ME-2 results.

1 Introduction

Atmospheric aerosols are generating increasing interest due to their adverse effects on human health, visibility and the climate (IPCC, 2013; Pope and Dockery, 2006). Among different particulate compositions, many studies focus on organic aerosols (OAs) because they contribute 20-90% to the total submicron mass (Jimenez et al., 2009; Zhang et al., 2007). OAs can be either directly emitted by various sources, including anthropogenic (i.e., traffic and combustion activities) and biogenic sources, or produced via secondary formation after the oxidation of volatile organic compounds (VOCs) (Hallquist et al., 2009).

¹ Correspondence to: X.-F. Huang (huangxf@pku.edu.cn)

27 Therefore, the reliable source identification and quantification of OAs are essential before developing effective political
28 abatement strategies.

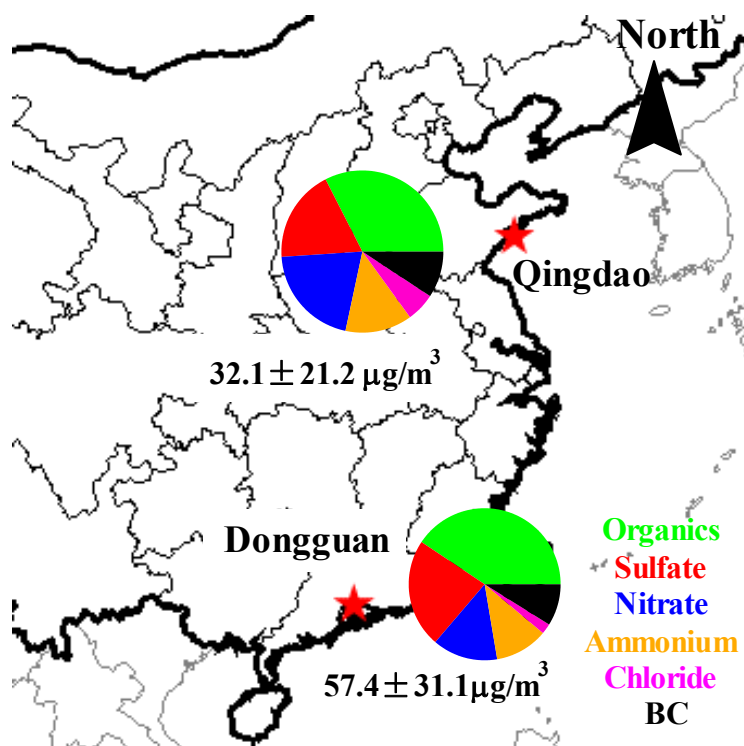
29 Aerodyne aerosol mass spectrometer (AMS) systems are the most widely adopted on-line aerosol measurement systems
30 for acquiring aerosol chemical compositions (Canagaratna et al., 2007; Pratt and Prather, 2012). An AMS provides on-line
31 quantitative mass spectra of non-refractory components from the submicron aerosol fraction with a high temporal resolution
32 (i.e., seconds to minutes) (Canagaratna et al., 2007). The total mass spectra can be assigned to both several inorganic
33 compounds and the organic fraction through mass spectral fragmentation tables (Allan et al., 2004). To further investigate the
34 different types of organic fractions, numerous studies have exploited the positive matrix factorization (PMF) algorithm and
35 apportioned the AMS organic mass spectra in terms of their source emissions or formation processes (Zhang et al., 2011).
36 PMF is a standard multivariate factor analysis tool (Paatero, 1999; Paatero and Tapper, 1994) that models the time series of
37 measured organic mass spectra as a linear combination of positive factor profiles and their respective time series. Most of the
38 earlier PMF studies were conducted on unit-mass resolution (UMR) mass spectrometers (Lanz et al., 2007; Lanz et al., 2010;
39 Ulbrich et al., 2009), although more have recently focused on high-resolution (HR) mass spectra PMF (Aiken et al., 2009;
40 Docherty et al., 2008; Huang et al., 2010). The use of HR mass spectra data to constrain PMF solutions can reduce their
41 rotational ambiguity and result in more interpretable OA factors. For example, Aiken et al. (2009) found that hydrocarbon-like
42 OA (HOA) and biomass burning OA (BBOA) were better separated using HR-AMS data than with UMR data. However, even
43 HR-AMS-PMF can also yield mixed factors (especially in heavily polluted areas) due to their complex emission patterns.

44 The abundant characteristic fragments for cooking-related OA (COA) (e.g., m/z 55 and 57) and coal combustion OA
45 (CCOA) (e.g., m/z 51, 53, and 65) can be observed in the mass spectrum of the HOA factor (He et al., 2010; Hu et al., 2013).
46 Elser et al., 2016) analyzed two urban HR-AMS datasets in China, and their PMF results showed an HOA profile that
47 contained a high concentration of $C_2H_4O_2^+$ (m/z 60), which is a BBOA tracer ion. In addition, CO_2^+ (m/z 44) contributed more
48 to COA compared to oxygenated OA (OOA). To solve this “mixed factor” problem in PMF analysis, some researchers
49 attempted to use the multilinear engine algorithm (ME-2) with user-provided constraints (Canonaco et al., 2013; Crippa et al.,
50 2014; Elser et al., 2016; Reyes-Villegas et al., 2016). However, several key issues with the ME-2 in these studies, such as
51 reliability of the user-input constraints and the criteria used to determine an optimal result, still require further investigation.
52 Most ME-2 studies (Crippa et al., 2014; Elser et al., 2016; Reyes-Villegas et al., 2016) were based on HR-AMS datasets and
53 utilized mass profiles of PMF results from Paris (Crippa et al., 2013; mostly due to the lack of other reliable source profiles)
54 and did not consider the specific sampling sites, which could result in uncertainties.

55 In this study, a novel source apportionment technique using the multi-linear engine tool (ME-2) was successfully applied
56 to organic mass spectra obtained with an HR-ToF-AMS at two urban sites during pollution-heavy periods during the same
57 year. The improved OA source apportionment results are discussed and compared with an unconstrained PMF analysis.

59 **2.1 Sampling sites and period**

60 Measurements at Qingdao (36.10°N, 120.47°E, 10 m above ground level, a.g.l.) were performed from 1 to 31 November
61 2013, while those in Dongguan were conducted from 12 December 2013 to 1 January 2014 (33.03°N, 113.75°E, 100 m a.g.l.).
62 Qingdao is a coastal city with over 9 million inhabitants in northern China, while Dongguan has over 8 million inhabitants and
63 is located in southern China (shown in Figure 1). Both of the sampling sites are on the tops of buildings in urban central areas,
64 and there is no industrial emission nearby.
65



66
67 **Figure 1.** The locations and the average PM₁ chemical compositions of the Qingdao and Dongguan sampling sites.
68

68 **2.2 Instrumentation**

69 An HR-ToF-AMS was deployed for the on-line measurement of non-refractory PM₁ (Canagaratna et al., 2007). The setup
70 and operation of the HR-ToF-AMS was similar to that in our previous studies (Huang et al., 2015; Huang et al., 2010). A PM_{2.5}
71 cyclone inlet was briefly placed on the roof of a building to remove coarse particles and to introduce an air stream containing
72 the remaining particles into a room through a copper tube with a flow rate of 10 l min^{-1} . A nafion dryer (MD-070-12S-4, Perma
73 Pure Inc.) was positioned upstream of the HR-ToF-AMS to eliminate the potential influence of relative humidity on the

74 particle collection (Matthew et al., 2008), after which the HR–ToF–AMS isokinetically sampled from the center of the copper
75 tube at a flow rate of 80 ml min⁻¹. The instrument was operated at two ion optical modes with a cycle of 4 min, including 2
76 min for the mass-sensitive V-mode and 2 min for the high mass resolution W-mode. An aethalometer (AE-31, Magee), which
77 also has a PM_{2.5} inlet, was simultaneously used for measurements of refractory black carbon (BC) with a temporal resolution
78 of 5 min.

79 A routine analysis of the HR–ToF–AMS data was performed using the software SQUIRREL (version 1.57) and PIKA
80 (version 1.16) written in Igor Pro 6.37 (Wave Metrics
81 Inc.)(<http://cires1.colorado.edu/jimenezgroup/ToFAMSResources/ToFSoftware/index.html>). The ionization efficiency (IE)
82 was calibrated using pure ammonium nitrate particles following standard protocols (Drewnick et al., 2005; Jayne et al.,
83 2000). The relative IEs (RIEs) for organics, nitrate and chloride were assumed to be 1.4, 1.1 and 1.3, respectively. A
84 composition-dependent collection efficiency (CE) was applied to the data based on the method of Middlebrook et al. (2012)
85 and an organic elemental analysis was performed using the latest approach recommended by Canagaratna et al. (2015).

86 **2.3 PMF and ME-2 methods for OA source apportionment**

87 PMF is a mathematical technique used to solve bilinear unmixing problems (Paatero and Tapper, 1994) that enables a
88 description of the variability of a multivariate database as the linear combination of static factor profiles and their
89 corresponding time series. The bilinear factor analytic model in matrix notation is defined in Eq. (1), where the measured
90 matrix X (consisting of i rows and j columns) is approximated by the product of G (containing the factor time series) and F
91 (the factor profiles). E denotes the model residuals. The entries in G and F are fitted using a least-squares algorithm that
92 iteratively minimizes the quantity Q (Eq. 2), which is defined as the sum of the squared residuals (e_{ij}) weighted by their
93 respective uncertainties (σ_{ij}).

$$94 \quad X = G \times F + E \quad (1)$$

$$95 \quad Q = \sum_{i=1}^m \sum_{j=1}^n \left(\frac{e_{ij}}{\sigma_{ij}} \right)^2 \quad (2)$$

96 In this study, we adopted SoFi (Canonaco et al., 2013), which is an implementation of the multilinear engine (ME-2)
97 (Paatero, 1999), to perform the organic HR-AMS data analysis. In contrast to an unconstrained PMF analysis, ME-2 enables
98 a more complete exploration of the rotational ambiguity of the solution space. In our case, this is achieved by directing the
99 solution towards environmentally meaningful rotations using the *a* value approach. This method uses prior input profiles and
100 the scalar *a* to constrain one or more output factor profiles such that they fall within a predetermined range. The *a* value
101 determines the extent to which the output profiles are allowed to vary from the input profiles according to Eq. (3), where *f*
102 represents the factor profile and *j* indicates the *m/z* of the ions.

$$103 \quad f_{j,\text{solution}} = f_j \pm a \times f_j \quad (3)$$

104 The number of output factors, which is selected by the user, is a key consideration for PMF analysis. Most unconstrained PMF
105 results were chosen following the procedures detailed in Zhang et al. (2007). However, additional outputs in ME-2 can be

106 generated to explore more of the solution space, and more criteria should be developed to support the factor identification,
107 which will be discussed in section 3.

108 **2.4 Polycyclic aromatic hydrocarbons (PAHs) quantification**

109 In this study, PAHs mass concentrations were quantitatively determined from the HR-AMS data. The steps outlined are
110 as follows: first, the PAHs molecular ions $[M]^+$, including $[C_{10}H_8]^+$, $[C_{12}H_8]^+$, $[C_{14}H_8]^+$, $[C_{14}H_{10}]^+$, $[C_{16}H_{10}]^+$, $[C_{18}H_{10}]^+$,
111 $[C_{18}H_{12}]^+$, $[C_{20}H_{12}]^+$, $[C_{22}H_{12}]^+$, $[C_{22}H_{14}]^+$, $[C_{24}H_{12}]^+$, $[C_{24}H_{14}]^+$, and other associated fragments, including $[M-H]^+$, $[M-2H]^+$,
112 $[M]^{2+}$, and $[M-H]^{2+}$ were fitted in the HR spectra. Second, the fragments presented low correlation (i.e., R^2 below 0.6) with
113 their corresponding molecular ions were not taken into account. Finally, the relative ionization efficiency (RIE) for PAHs was
114 assumed to be 1.4 and the dependency of the collection efficiency (CE_b) on the chemical composition of the aerosol was
115 estimated using a composition-dependent collection efficiency (CDCE) algorithm (Middlebrook et al., 2012). More details
116 about the method can be found in Bruns et al. (2015).

117 **3 Interpretation of OA source apportionment using ME-2**

118 In this section, a conventional PMF without any prior information is performed to analyze the OA source apportionment.
119 Then, we use the ME-2 method to optimize the OA source apportionment based on the information obtained from the PMF
120 method. The sequential steps are reported below:

121 1. Unconstrained PMF runs.

122 We performed unconstrained runs with a range from two to ten factors. Generally, PMF solutions with large numbers of
123 factors are not considered due to possible mathematical splits of the factor profiles. However, some factors that have small
124 contributions or that have similar mass profiles as other factors (but different time series) may only be found in solutions with
125 large numbers of factors. We observe that most of the solutions provided via PMF include either multiply split factors or mixed
126 factors that are not properly separated from one another. In other words, PMF does not produce an appropriate solution. The
127 6-factor solutions for Qingdao and Dongguan are shown in Figure S1 and S2, and three types of primary OAs (POAs) were
128 identified for each sampling site, including HOA), coal combustion OA (CCOA) and cooking OA (COA) for Qingdao and
129 HOA, biomass burning OA (BBOA) and COA for Dongguan. Oxygenated OA (OOA) seems to be excessively split in the 6-
130 factor solutions for both of the sites. HOA is distinguished by alkyl fragment signatures with prominent contributions of m/z
131 55 ($C_4H_7^+$) and m/z 57 ($C_4H_9^+$) (Ng et al., 2011). The COA profile is similar to that of HOA but has a higher contribution from
132 oxygenated ions at m/z 55 ($C_3H_3O^+$) and m/z 57 ($C_3H_5O^+$) (Mohr et al., 2012). BBOA is characterized by the presence of
133 signals at m/z 60 ($C_2H_4O_2^+$) and m/z 73 ($C_3H_5O_2^+$), which are identified as fragments from anhydrous sugars present in biomass
134 smoke (Alfarra et al., 2007). The OOA profile is characterized by a high signal at m/z 44 (CO_2^+). Note that some POA profiles
135 in this solution indicate mixing; for example, CCOAs in Qingdao contain a high concentration of the biomass burning tracer
136 ion (m/z 60, $C_2H_4O_2^+$), and HOAs in Dongguan have a higher-than-expected contribution of m/z 44 (CO_2^+) with a high O/C

137 ratio (0.26). In addition, CCOA seems to be mixed with BBOA. We then further verified the solutions with additional factors.
138 The results show that BBOA and CCOA are separated from each other in the 7- and 8-factor solutions for Qingdao (see Figure
139 S1) and that better signals for unmixed and stable HOA with low O/C ratios of 0.17 or 0.18 emerged in the 7- to 10-factor
140 solutions for Dongguan (see Figure S2).

141 2. Investigate anchor profiles for ME-2.

142 Before operating ME-2, feasible and reasonable prior input profiles must be determined. To the best of our knowledge,
143 this is the first HR-OA data set that employs anchor profiles extracted from an unconstrained PMF solution with a higher
144 number of factors, and the same approach has been successfully applied to source apportionment efforts using UMR ME-2
145 (Fröhlich et al., 2015). In our case for Qingdao, the BBOA anchor profile should be investigated, and we attempted to look for
146 it from the unconstrained PMF results based on the same dataset, and found that the BBOA factors in the 7- and 8-factor
147 solutions might be used as the anchor profiles. They both had good correlation with the BBOA MS in Chinese biomass burning
148 emission simulation (He et al., 2010), confirming their basic BBOA characteristics. Although these two BBOA factors are
149 quite similar, the BBOA from the 8-factor solution is better suited to be a constraining profile due to its smaller m/z 44 (CO_2^+)
150 signal and higher m/z 60 ($\text{C}_2\text{H}_4\text{O}_2^+$) signal (see Figure S3). In addition, the BBOA from the 8-factor solution also correlates
151 better with the BBOA from a Chinese biomass burning simulation ($R^2=0.81$) than the 7-factor solution ($R^2=0.79$). For
152 Dongguan, the anchor profile for HOA can be obtained from unconstrained PMF solutions. The averaged HOA profile from
153 the 7- to 10-factor solutions was used as the anchor profile for ME-2 due to the small differences among the different solutions.
154 Additionally, the constraining CCOA profile for Dongguan is still under consideration because the mass spectrum of BBOA
155 was found to be very similar to that of CCOA, raising the concern that coal combustion particles might have been incorrectly
156 apportioned to biomass burning sources (Wang et al., 2013). An appropriate CCOA anchor profile could not be obtained due
157 to an increase in the unconstrained PMF factor number (see Figure S2). The best approach is to employ the CCOA profile
158 from Qingdao as the constraining profile for Dongguan in ME-2, as these two campaigns were conducted using the same HR-
159 ToF-AMS in the same year. In addition, the CCOA from Qingdao has a very good correlation ($R^2=0.97$) with CCOA profiles
160 reported at other Chinese urban sites (Elser et al., 2016) (see Figure S4). Tian et al. (2012) also found that the emission
161 compositions of coal combustion in different regions in China are quite similar. The input profiles for BBOA, HOA and CCOA
162 prior to operating ME-2 are shown in Figure 2.

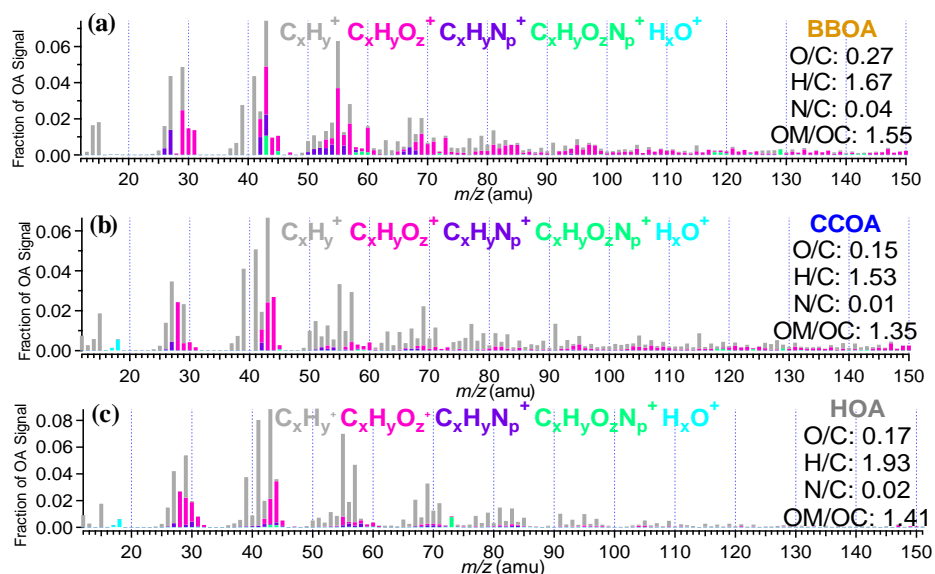


Figure 2. The anchor mass spectra for (a) BBOA, (b) CCOA and (c) HOA in the ME-2 analysis.

3. Constrain the mass spectrums of the mixed factors with different a values.

According to the unconstrained PMF results, the best interpretable results for both two sites are the 6-factor solutions with factors that include HOA, COA, BBOA, CCOA, less-oxidized oxygenated OA (LO-OOA) and more-oxidized oxygenated OA (MO-OOA) (Figure 3a and 3b). The a values set from 0 to 1 with an increment of 0.1 for BBOA in Qingdao yields 11 possible solutions, and for both HOA and CCOA in Dongguan yields 121 possible solutions.

4. Criteria for obtaining the optimal results.

In this study, we used two simple and reasonable criteria to obtain a better environmental OA source apportionment: the reasonability of the O/C ratio and the correlation between the factors and the tracers. For Qingdao, the O/C ratios for six resolved factors and the correlations between CCOA and PAHs, HOA and BC for 11 solutions with different a values are shown in Table S2. These results indicate that all of the O/C ratios for each factor and each factor-tracer correlation are quite similar to one another and that they agree with the range of values in the literature (Canagaratna et al., 2015). Therefore, the solutions averaged over the 11 outputs were considered the final results for Qingdao. For Dongguan, all of the O/C ratios for HOA, CCOA, COA and BBOA among the 121 possible solutions are listed in Table S3. The O/C ratio of HOA in the unconstrained PMF results remained between approximately 0.17 and 0.18, providing a filter criterion with which to assess reasonable ME-2 solutions, and only solutions with a values between 0 and 0.1 fell into this range (Table S1). The O/C ratios of other factors for a values between 0 and 0.1 are shown in Table S3. The solutions using a values between 0 and 0.1 for the HOA profile and an a value of 0.9 for the CCOA profile are considered ideal results for three reasons. First, unlike the HOA mass spectra, CCOAs from different sites show higher variability and the CCOA anchor profile is not derived from itself, and therefore, it is reasonable to restrict the constraint with small a values for HOA and a looser constraint should be applied for CCOA, which is consistent with the a values selecting rules in London ME-2 study (Reyes-Villegas et al., 2016). Second, the

186 POA factors in Dongguan, including HOA and CCOA, have higher O/C ratios likely as a result of a higher atmospheric
187 oxidizing capacity and a stronger photochemical formation in Southern China (Hofzumahaus et al., 2009). Moreover, some
188 studies reported that BBOAs undergo substantial chemical processing immediately after emission and that aged BBOAs had
189 significant concentrations in fresh plumes (Zhou et al., 2017). Thus, CCOAs in Dongguan are very likely to demonstrate
190 relatively higher ages than those in Qingdao (0.15) with higher O/C ratios (but with an O/C ratio of up to 1.25 when the α
191 value is 1, which is unacceptable). Third, with an increase in the α value for CCOA, two types of OOA become more
192 distinctive, and the factor correlates better with the tracer (Table S1 and Table S4).

193 In order to prove the improvement of using the anchor profiles generated by the unconstrained PMF run with the same
194 local datasets, we also run the ME-2 analysis using the anchor profiles available in the literature, with the results shown in
195 Table S5 and S6. For Qingdao, the correlations between POAs and their tracers and the Q/Q_{exp} values using the three BBOA
196 profiles in the literature are poorer than using the BBOA obtained in this study (Table S5). For Dongguan, the results from
197 ME-2 using the HOA profiles in the literature are also poorer than using the HOA profiles obtained in this study (Table S6).
198 Therefore, it can be clearly seen that the method to obtain an anchor profile in this study is easier (it does not depend on the
199 results in the literature) and more valid.

200 **4 Results and discussion**

201

202 **4.1 Variations in the OA factors**

203 Figure 1 shows the chemical compounds of PM₁, including the non-refractory (NR) components measured via HR-AMS
204 (i.e., OA, SO₄, NO₃, NH₄ and Cl) and BC concentrations measured via the AE-31, during the sampling period in both Qingdao
205 and Dongguan. The average PM₁ mass concentration was 32.1±21.2 μg/m³ (mean ± standard deviation) in Qingdao and
206 57.4±31.1 μg/m³ in Dongguan. The temporal variations in the PM₁ species in conjunction with meteorological parameters are
207 shown in Figure S5. Although Dongguan is located in southern China with relatively less air pollution (Huang et al., 2012),
208 the PM₁ mass concentration was higher. This is mainly because of stagnant meteorological conditions with low average wind
209 speeds (i.e., 2.3 m/s) and a maximum wind speed of less than 6 m/s. Among the PM₁ compounds, OAs accounted for 32.5%
210 of PM₁ in Qingdao and 40.6% in Dongguan. This suggests that OA constitutes a very important fraction at both urban sites.
211 Thus, the final and detailed results of the OA source apportionment are presented in this section.

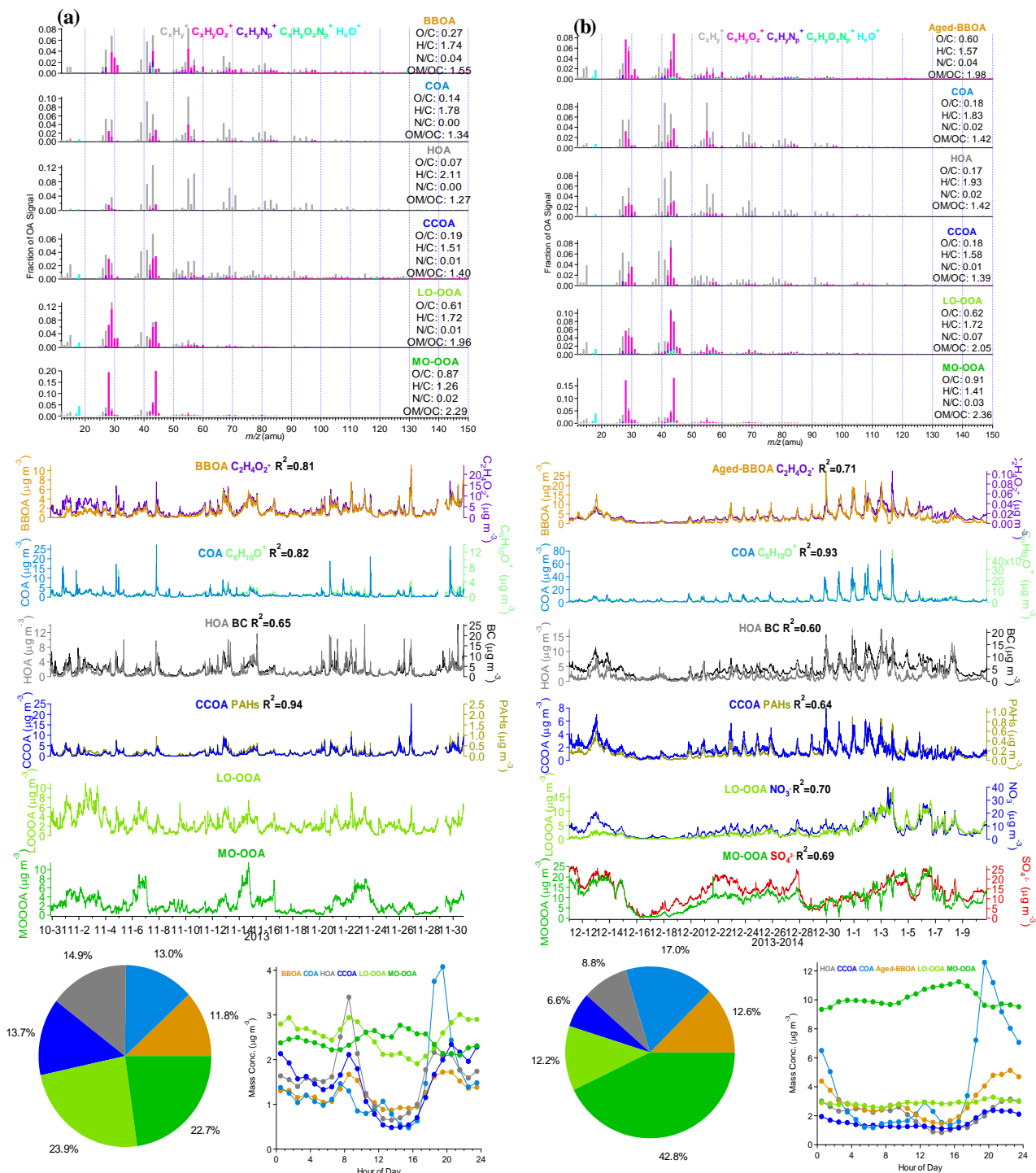
212 For Qingdao, the final result is the average of all of the ME-2 runs with constraints including α values from 0 to 1 fulfilling
213 the criteria described in section 3.2. The mass spectra and time series of the resolved OA sources are shown in Figure 3a. The
214 characteristics of each factor were distinct. The BBOA profile contained the highest m/z 60 fraction f_{60} (1.5%) compared to
215 the other factors, and the concentrations were highly correlated with C₂H₄O₂⁺ (R²=0.81). The mass spectra of COA was
216 characterized by a high m/z 55/57 ratio, which is consistent with previous results (He et al., 2010; Mohr et al., 2012; Sun et al.,

217 2016). In addition, the time series of COA showed a good correlation with its tracer ion $C_6H_{10}O^+$ in accordance with (Sun et
218 al., 2016). HOAs were correlated well with BC ($R^2=0.65$), and CCOAs were highly correlated with PAHs ($R^2=0.94$). Among
219 the two types of OOAs, the less-oxidized OOA (LO-OOA) had a lower CO_2^+ fraction and O/C ratio (0.62) compared with the
220 more oxidized OOA (MO-OOA), which had a higher CO_2^+ fraction and O/C (0.91) ratio. The sum of LO-OOA and MO-OOA
221 showed a high correlation with the sum of sulfate and nitrate ($R^2=0.76$). The POAs (including HOA, COA, BBOA and CCOA)
222 contributed 53.4% to the OA concentration (Figure 3a), which was almost equal to the SOA fraction. In terms of the diurnal
223 trends of the OA factors shown in Figure 3a, they are all partially driven both by PBL dynamics (demonstrating an increased
224 dilution during the daytime and an accumulation of particulate matter overnight) and by the diurnal emission profile. The
225 diurnal trend of HOA showed pronounced peaks during the morning and evening rush hours (8:00-9:00 and 19:00-21:00),
226 which is typically the case for traffic-related pollutants. COA shows a very distinct daily trend with strong peaks during the
227 lunch (approximately 12:00) and dinner (19:00-20:00) periods. CCOAs constituted an important and dominant source of
228 pollutants during the wintertime in northern Chinese areas (Elser et al., 2016) due to heating activities, especially with regard
229 to the central-heating supply that began on November 13 and continued until the end of the campaign. The diurnal variations
230 of the four POA factors before and during the central-heating period are shown in Figure S6. In comparison with the other
231 three POAs, the diurnal pattern of CCOA showed a clear increase during the central-heating period with concentration peaks
232 during the morning (at approximately 9:00) and at night (starting to rise at 18:00), which seems consistent with heating
233 emissions and atmospheric dilution. The diurnal trends of BBOA were similar to those of CCOA. The dilution of these particles
234 within a deeper PBL during the daytime resulted in a decreasing trend in the BBOA concentration, while peaks related to
235 residential heating were observed during the morning (between 09:00 to 10:00) and at night (starting to rise at 17:00). The
236 main difference between the LO-OOA and MO-OOA diurnal patterns is that an increase in the MO-OOA mass concentration
237 was observed during the daytime, implying that the formation of secondary organic aerosols was greatly enhanced during the
238 afternoon. In addition, the diurnal cycle for LO-OOA showed a relatively smaller decrease during the daytime compared with
239 the POA factors. These characteristics of the OOA diurnal trend confirm their secondary nature.

240 For Dongguan, similar to the OA source apportionment using ME-2 in Qingdao, the final result is the average of two
241 accepted a-value solutions with six identified factors, including HOA, CCOA, COA, Aged-BBOA, LO-OOA and MO-OOA.
242 Although the range of the O/C ratio of BBOA reported in Canagaratna et al. (2015) was from 0.25 to 0.55, fresh BBOA was
243 found to be rapidly converted to OOA in less than 1 day (Bougiatioti et al., 2014), and the O/C ratio of aged BBOA could be
244 up to 0.85 (Zheng et al., 2017). BBOA in Dongguan was apparently not fresh considering it is an urban site and Dongguan has
245 a warmer winter (17 °C in Dongguan vs. 9 °C in Qingdao). The BBOA factor identified in Dongguan, with a strong contribution
246 of m/z 60, had a higher O/C, indicating it was an oxygenated BBOA, therefore we name it Aged-BBOA in this study. All of
247 the information regarding the final source results is shown in Figure 3b. Good correlations between each OA factor and their
248 tracers indicate that the resolved ME-2 results are reasonable. A few sharp drops (which always occurred at approximately
249 20:00) were observed in the MO-OOA time series ranging from December 29 to January 5, which coincides with extreme
250 organic aerosol pollution (Figure S5). The inherent mechanisms for these drops remain unexplained, although we have tried a

251 number of reasonable approaches (e.g., splitting the period into sub-periods to identify the sources, constraining more factors
252 before running ME-2, and examining more factors) to address this issue. A similar problem in the MO-OOA time series was
253 also found in a recent ME-2 application (Qin et al., 2017). In our case, we presume this might be the result of relatively worse
254 meteorological conditions at night during the sampling period, thereby increasing the contribution of late supper emissions
255 and leading to the overestimation of COAs offset by drops in the MO-OOA concentration. Also note that the O/C ratios of the
256 POAs in Dongguan were higher than those in Qingdao, suggesting that POA emissions in Dongguan underwent faster chemical
257 processing. In addition, the relatively smaller contributions of POAs further support this inference. Freshly emitted POAs may
258 get mixed with aged OAs more easily, while ME-2 may still consider them unmixed. MO-OOAs accounted for an average of
259 42.8% of the total OA mass (which is much greater than the contribution of LO-OOAs), which is probably because some POA
260 species could have been rapidly converted to very aged OOs (Bougiatioti et al., 2014; Xu et al., 2015). As mentioned above,
261 the characteristics of the diurnal trends of the POA factors in Dongguan were similar to those in Qingdao, and thus, we focused
262 on the OOA factors. MO-OOAs still showed higher concentrations during the daytime but, unlike LO-OOAs in Qingdao, the
263 diurnal patterns of LO-OOAs in Dongguan were flat, implying that secondary OA formation in the LO-OOAs basically offset
264 the influences of PBL variations.

265 Meteorological conditions (especially wind) play a crucial role in the dilution and transport of air pollution. We used the
266 relationships between the component concentrations and wind to profoundly understand the origins of the OA factors and their
267 nature. The distributions of the OA factor concentrations versus the wind direction and speed are plotted in Figure S7. For
268 both of the urban sites, higher mass concentrations of the POA factors were mostly accompanied by low wind speeds, denoting
269 their local emission characteristics. Additionally, for the OOA factors, a large proportion of their higher concentrations were
270 maintained at higher wind speeds, indicating that the OOs were formed by transport processes. However, the small fraction
271 of high-level OOs that was concentrated within the low wind-speed region represents the fast formation of OOs from some
272 local POA.



273

274

275

Figure 3. Mass spectra of the OA factors, average fractions of the OA factors, diurnal variations of the OA factors and time series of the OA factors identified by the ME-2 method for (a)Qingdao and (b) Dongguan.

4.2 Regression analysis for POA tracers

278 BC and PAHs are mainly derived from incomplete combustion processes (Schmidt and Noack, 2000; White, 1985), and
279 thus, they were used as tracers for the POAs. In this study, the BC was directly measured by the AE-31, and the PAHs were
280 quantified using the method developed by Bruns et al. (2015) based on AMS data. Both the BC and PAHs showed pronounced
281 diurnal cycles similar to those of the POAs (see Figure S8). In addition, POAs are properly split into different subtypes via the
282 ME-2 method, thereby providing the possibility to better understand the contributions of different POAs to BC and PAHs and
283 to verify the POA source identification. In this section, we use a multi-linear regression method to analyze the POA factors for
284 BC and PAHs.

285 Figure 4 shows the average contributions of OA sources to BC and PAHs in Qingdao and Dongguan. At both sites, HOAs
286 were the dominant attribute of BC (51% for Qingdao and 40% for Dongguan) and CCOAs contributed the most to the PAHs
287 (59% for Qingdao and 43% for Dongguan), indicating that BC mainly originates from traffic emissions and that PAHs in the
288 Chinese urban polluted atmosphere are dominated by coal combustion during the wintertime. These findings are consistent
289 with results reported in similar studies (Elser et al., 2016; Huang et al., 2015; Huang et al., 2010; Sun et al., 2016; Xu et al.,
290 2014; Zhang et al., 2008). Moreover, the ratio of PAHs to OAs (1.8%) in Qingdao was similar to that in the northern Chinese
291 urban site of Xi'an (1.9%) (Elser et al., 2016) but was higher than that in Dongguan (0.9%). This is likely because a larger
292 fraction of coal combustion to the total OA concentration would enhance the ratio of PAHs to OAs (Elser et al., 2016). Biomass
293 burning was the second-most important source for both BC and PAHs; it was responsible for 33% and 29% of the BC at
294 Qingdao and Dongguan, respectively, and for 29% and 34% of the PAHs at Qingdao and Dongguan, respectively. Cooking
295 emissions were a minor source of BC and PAHs, accounting for less than 10%. These results are also consistent with the
296 published findings. For example, biomass burning is an important source for BC (Kondo et al., 2011; Reddy et al., 2002) and,
297 in some regions with fewer traffic emissions, BC has the best correlation with BBOAs (Schwarz et al., 2008). In addition, in
298 Beijing and California, PAHs are correlated well with BBOAs but are much more weakly correlated with COAs (Ge et al.,
299 2012; Hu et al., 2016; Sun et al., 2016).

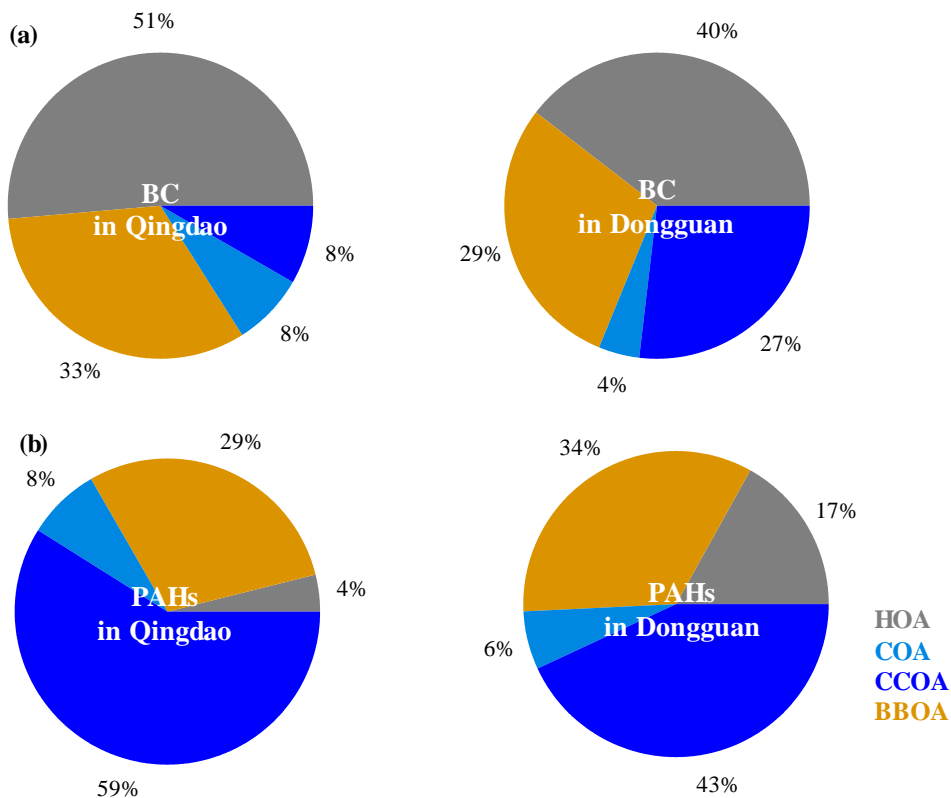


Figure 4. (a) Average contributions of POA factors to BC; (b) average contributions of POA factors to PAHs.

5 Conclusions

In this study, we used PMF to interpret the organic aerosol sources at two Chinese urban sites in winter, and found that PMF did not work properly (i.e., it did not allow for the separation of several primary sources of OAs). Therefore, we adopted the ME-2 approach, which yields more reliable solutions. Technically, there are three important steps when using the ME-2 method to interpret the sources of OAs. The first step is to investigate the mixed and unidentified factors that are constrained according to issues in the unconstrained PMF results. Generally, we constrained one or more POA factors (i.e., HOA, COA, BBOA and CCOA) for the polluted urban sites. The second step is to search for a reasonable anchor profile for each constrained factor. Two approaches were used: searching for anchor profiles via an increase in the number of unconstrained PMF factors from the same data set and using mass profiles derived from other similar studies. The third step is to choose the criteria for obtaining the optimal results. The choice of a reasonable range of O/C ratios may represent a good criterion for HR-OA apportionment since the O/C ratio is a significant and distinctive characteristic for different OA factors. In addition, correlations between the resolved OA factors and their tracers were also suggested.

314 **Acknowledgments**

315 This work was supported by the National Natural Science Foundation of China (91744202, 41622304) and the Science and
316 Technology Plan of Shenzhen Municipality (JCYJ20170412150626172, JCYJ20170306164713148).

317 **References**

- 318 Aiken, A. C., D. Salcedo, M. J. Cubison, J. A. Huffman, P. F. DeCarlo, I. M. Ulbrich, K. S. Docherty, D. Sueper, J. R.
319 Kimmel, D. R. Worsnop, A. Trimborn, M. Northway, E. A. Stone, J. J. Schauer, R. M. Volkamer, E. Fortner, B. de Foy,
320 J. Wang, A. Laskin, V. Shutthanandan, J. Zheng, R. Zhang, J. Gaffney, N. A. Marley, G. Paredes-Miranda, W. P. Arnott,
321 L. T. Molina, G. Sosa, and J. L. Jimenez : Mexico City aerosol analysis during MILAGRO using high resolution aerosol
322 mass spectrometry at the urban supersite (T0) – Part 1: Fine particle composition and organic source apportionment,
323 *Atmos. Chem. Phys.*, 9(17), 6633-6653, doi: 10.5194/acp-9-6633-2009,2009.
- 324 Alfarra, M. R., A. S. H. Prevot, S. Szidat, J. Sandradewi, S. Weimer, V. A. Lanz, D. Schreiber, M. Mohr, and U.
325 Baltensperger : Identification of the Mass Spectral Signature of Organic Aerosols from Wood Burning Emissions,
326 *Environ Sci. Technol.*, 41(16), 5770-5777, doi: 10.1021/es062289b,2007.
- 327 Allan, J. D., A. E. Delia, H. Coe, K. N. Bower, M. R. Alfarra, J. L. Jimenez, A. M. Middlebrook, F. Drewnick, T. B. Onasch,
328 M. R. Canagaratna, J. T. Jayne, and D. R. Worsnop: A generalised method for the extraction of chemically resolved mass
329 spectra from Aerodyne aerosol mass spectrometer data, *J. Aerosol Sci.*, 35(7), 909-922, doi:
330 <https://doi.org/10.1016/j.jaerosci.2004.02.007>,2004.
- 331 Bougiatioti, A., I. Stavroulas, E. Kostenidou, P. Zarnmpas, C. Theodosi, G. Kouvarakis, F. Canonaco, A. S. H. Prévôt, A.
332 Nenes, S. N. Pandis, and N. Mihalopoulos : Processing of biomass-burning aerosol in the eastern Mediterranean during
333 summertime, *Atmos. Chem. Phys.*, 14(9), 4793-4807, doi: 10.5194/acp-14-4793-2014,2014.
- 334 Bruns, E. A., M. Krapf, J. Orasche, Y. Huang, R. Zimmermann, L. Drinovec, G. Močnik, I. El-Haddad, J. G. Slowik, J.
335 Dommen, U. Baltensperger, and A. S. H. Prévôt : Characterization of primary and secondary wood combustion products
336 generated under different burner loads, *Atmos. Chem. Phys.*, 15(5), 2825-2841, doi: 10.5194/acp-15-2825-2015,2015.
- 337 Canagaratna, M. R., J. L. Jimenez, J. H. Kroll, Q. Chen, S. H. Kessler, P. Massoli, L. Hildebrandt Ruiz, E. Fortner, L. R.
338 Williams, K. R. Wilson, J. D. Surratt, N. M. Donahue, J. T. Jayne, and D. R. Worsnop : Elemental ratio measurements of
339 organic compounds using aerosol mass spectrometry: characterization, improved calibration, and implications, *Atmos.*
340 *Chem. Phys.*, 15(1), 253-272, doi: 10.5194/acp-15-253-2015,2015.
- 341 Canagaratna, M. R., J. T. Jayne, J. L. Jimenez, J. D. Allan, M. R. Alfarra, Q. Zhang, T. B. Onasch, F. Drewnick, H. Coe, A.
342 Middlebrook, A. Delia, L. R. Williams, A. M. Trimborn, M. J. Northway, P. F. DeCarlo, C. E. Kolb, P. Davidovits, and
343 D. R. Worsnop : Chemical and microphysical characterization of ambient aerosols with the aerodyne aerosol mass
344 spectrometer, *Mass Spectrom. Rev.*, 26(2), 185-222, doi: 10.1002/mas.20115,2007.

345 Canonaco, F., M. Crippa, J. G. Slowik, U. Baltensperger, and A. S. H. Prévôt : SoFi, an IGOR-based interface for the
346 efficient use of the generalized multilinear engine (ME-2) for the source apportionment: ME-2 application to aerosol
347 mass spectrometer data, *Atmos. Meas. Tech.*, 6(12), 3649-3661, doi: 10.5194/amt-6-3649-2013,2013.

348 Crippa, M., DeCarlo, P. F., Slowik, J. G., Mohr, C., Heringa, M.F., Chirico, R., Poulain, L., Freutel, F., Sciare, J., Cozic, J.,
349 DiMarco, C. F., Elsasser, M., José, N., Marchand, N., Abidi, E., Wiedensohler, A., Drewnick, F., Schneider, J.,
350 Borrmann, S., Nemitz, E., Zimmermann, R., Jaffrezo, J.-L., Prévôt, A. S. H., and Baltensperger, U.: Wintertime aerosol
351 chemical composition and source apportionment of the organic fraction in the metropolitan area of Paris, *Atmos. Chem.*
352 *Phys.*, 13, 961–981, doi:10.5194/acp-13-961-2013, 2013.

353 Crippa, M., F. Canonaco, V. a. Lanz, M. Äijälä, J. D. Allan, S. Carbone, G. Capes, D. Ceburnis, M. Dall'Osto, D. A. Day, P.
354 F. DeCarlo, M. Ehn, a. Eriksson, E. Freney, L. Hildebrandt Ruiz, R. Hillamo, J. L. Jimenez, H. Junninen, A. Kiendler-
355 Scharr, A. M. Kortelainen, M. Kulmala, A. Laaksonen, A. A. Mensah, C. Mohr, E. Nemitz, C. O'Dowd, J. Ovadnevaite,
356 S. N. Pandis, T. Petäjä, L. Poulain, S. Saarikoski, K. Sellegri, E. Swietlicki, P. Tiitta, D. R. Worsnop, U. Baltensperger,
357 and A. S. H. Prévôt: Organic aerosol components derived from 25 AMS data sets across Europe using a consistent ME-2
358 based source apportionment approach, *Atmos. Chem. Phys.*, 14(12), 6159-6176, doi: 10.5194/acp-14-6159-2014, 2014.

359 Docherty, K. S., E. A. Stone, I. M. Ulbrich, P. F. DeCarlo, D. C. Snyder, J. J. Schauer, R. E. Peltier, R. J. Weber, S. M.
360 Murphy, J. H. Seinfeld, B. D. Grover, D. J. Eatough, and J. L. Jimenez : Apportionment of Primary and Secondary
361 Organic Aerosols in Southern California during the 2005 Study of Organic Aerosols in Riverside (SOAR-1), *Environ*
362 *Sci. Technol.*, 42(20), 7655-7662, doi: 10.1021/es8008166,2008.

363 Drewnick, F., S. S. Hings, P. DeCarlo, J. T. Jayne, M. Gonin, K. Fuhrer, S. Weimer, J. L. Jimenez, K. L. Demerjian, S.
364 Borrmann, and D. R. Worsnop : A New Time-of-Flight Aerosol Mass Spectrometer (TOF-AMS)—Instrument
365 Description and First Field Deployment, *Aerosol Sci. Tech.*, 39(7), 637-658, doi: 10.1080/02786820500182040,2005.

366 Elser, M., R. J. Huang, R. Wolf, J. G. Slowik, Q. Wang, F. Canonaco, G. Li, C. Bozzetti, K. R. Daellenbach, Y. Huang, R.
367 Zhang, Z. Li, J. Cao, U. Baltensperger, I. El-Haddad, and A. S. H. Prévôt : New insights into PM_{2.5} chemical
368 composition and sources in two major cities in China during extreme haze events using aerosol mass spectrometry,
369 *Atmos. Chem. Phys.*, 16(5), 3207-3225, doi: 10.5194/acp-16-3207-2016,2016.

370 Fröhlich, R., V. Crenn, A. Setyan, C. A. Belis, F. Canonaco, O. Favez, V. Riffault, J. G. Slowik, W. Aas, M. Äijälä, A.
371 Alastuey, B. Artiñano, N. Bonnaire, C. Bozzetti, M. Bressi, C. Carbone, E. Coz, P. L. Croteau, M. J. Cubison, J. K.
372 Esser-Gietl, D. C. Green, V. Gros, L. Heikkinen, H. Herrmann, J. T. Jayne, C. R. Lunder, M. C. Minguillón, G. Močnik,
373 C. D. O'Dowd, J. Ovadnevaite, E. Petralia, L. Poulain, M. Priestman, A. Ripoll, R. Sarda-Estève, A. Wiedensohler, U.
374 Baltensperger, J. Sciare, and A. S. H. Prévôt : ACTRIS ACSM intercomparison – Part 2: Intercomparison of ME-2
375 organic source apportionment results from 15 individual, co-located aerosol mass spectrometers, *Atmos. Meas. Tech.*,
376 8(6), 2555-2576, doi: 10.5194/amt-8-2555-2015,2015.

377 Ge, X., A. Setyan, Y. Sun, and Q. Zhang : Primary and secondary organic aerosols in Fresno, California during wintertime:
378 Results from high resolution aerosol mass spectrometry, *J. Geophys. Res.-Atmos.*, 117(D19), 161-169, doi:
379 10.1029/2012JD018026,2012.

380 Hallquist, M., J. C. Wenger, U. Baltensperger, Y. Rudich, D. Simpson, M. Claeys, J. Dommen, N. M. Donahue, C. George,
381 A. H. Goldstein, J. F. Hamilton, H. Herrmann, T. Hoffmann, Y. Iinuma, M. Jang, M. E. Jenkin, J. L. Jimenez, A.
382 Kiendler-Scharr, W. Maenhaut, G. McFiggans, T. F. Mentel, A. Monod, A. S. H. Prévôt, J. H. Seinfeld, J. D. Surratt, R.
383 Szmigielski, and J. Wildt : The formation, properties and impact of secondary organic aerosol: current and emerging
384 issues, *Atmos. Chem. Phys.*, 9(14), 5155-5236, doi: 10.5194/acp-9-5155-2009,2009.

385 He, L. Y., Y. Lin, X. F. Huang, S. Guo, L. Xue, Q. Su, M. Hu, S. J. Luan, and Y. H. Zhang : Characterization of high-
386 resolution aerosol mass spectra of primary organic aerosol emissions from Chinese cooking and biomass burning,
387 *Atmos. Chem. Phys.*, 10(23), 11535-11543, doi: 10.5194/acp-10-11535-2010,2010.

388 Hofzumahaus, A., F. Rohrer, K. Lu, B. Bohn, T. Brauers, C.-C. Chang, H. Fuchs, F. Holland, K. Kita, Y. Kondo, X. Li, S.
389 Lou, M. Shao, L. Zeng, A. Wahner, and Y. Zhang : Amplified Trace Gas Removal in the Troposphere, *Science*,
390 324(5935), 1702, doi: 10.1126/science.1164566,2009.

391 Hu, W., M. Hu, W. Hu, J. L. Jimenez, B. Yuan, W. Chen, M. Wang, Y. Wu, C. Chen, Z. Wang, J. Peng, L. Zeng, and M.
392 Shao : Chemical composition, sources, and aging process of submicron aerosols in Beijing: Contrast between summer
393 and winter, *J. Geophys. Res.-Atmos.*, 121(4), 1955-1977, doi: 10.1002/2015JD024020,2016.

394 Hu, W. W., M. Hu, B. Yuan, J. L. Jimenez, Q. Tang, J. F. Peng, W. Hu, M. Shao, M. Wang, L. M. Zeng, Y. S. Wu, Z. H.
395 Gong, X. F. Huang, and L. Y. He: Insights on organic aerosol aging and the influence of coal combustion at a regional
396 receptor site of central eastern China, *Atmos. Chem. Phys.*, 13(19), 10095-10112, doi: 10.5194/acp-13-10095-2013,2013.

397 Huang, R. J., Y. Zhang, C. Bozzetti, K. F. Ho, J. J. Cao, Y. Han, K. R. Daellenbach, J. G. Slowik, S. M. Platt, F. Canonaco,
398 P. Zotter, R. Wolf, S. M. Pieber, E. A. Brunts, M. Crippa, G. Ciarelli, A. Piazzalunga, M. Schwikowski, G. Abbaszade, J.
399 Schnelle-Kreis, R. Zimmermann, Z. An, S. Szidat, U. Baltensperger, I. El Haddad, and A. S. H. Prévôt: High secondary
400 aerosol contribution to particulate pollution during haze events in China, *Nature*, 514(7521), 218-222, doi:
401 10.1038/nature13774,2015.

402 Huang, X. F., L. Y. He, L. Xue, T. L. Sun, L. W. Zeng, Z. H. Gong, M. Hu, and T. Zhu: Highly time-resolved chemical
403 characterization of atmospheric fine particles during 2010 Shanghai World Expo, *Atmos. Chem. Phys.*, 12(11), 4897-
404 4907, doi: 10.5194/acp-12-4897-2012,2012.

405 Huang, X. F., L. Y. He, M. Hu, M. R. Canagaratna, Y. Sun, Q. Zhang, T. Zhu, L. Xue, L. W. Zeng, X. G. Liu, Y. H. Zhang,
406 J. T. Jayne, N. L. Ng, and D. R. Worsnop : Highly time-resolved chemical characterization of atmospheric submicron
407 particles during 2008 Beijing Olympic Games using an Aerodyne High-Resolution Aerosol Mass Spectrometer, *Atmos.*
408 *Chem. Phys.*, 10(18), 8933-8945, doi: 10.5194/acp-10-8933-2010,2010.

409 IPCC , Climate Change 2013: The Physical Science Basis. Contribution of Working Group I to the Fifth Assessment Report
410 of the Intergovernmental Panel on Climate Change, 1535 pp., Cambridge University Press, Cambridge, United Kingdom
411 and New York, NY, USA,2013.

412 Jayne, J. T., D. C. Leard, X. Zhang, P. Davidovits, K. A. Smith, C. E. Kolb, and D. R. Worsnop :Development of an Aerosol
413 Mass Spectrometer for Size and Composition Analysis of Submicron Particles, *Aerosol Sci. Tech.*, 33(1-2), 49-70, doi:
414 10.1080/027868200410840,2000.

415 Jimenez, J. L., M. R. Canagaratna, N. M. Donahue, A. S. H. Prevot, Q. Zhang, J. H. Kroll, P. F. DeCarlo, J. D. Allan, H.
416 Coe, N. L. Ng, A. C. Aiken, K. S. Docherty, I. M. Ulbrich, A. P. Grieshop, A. L. Robinson, J. Duplissy, J. D. Smith, K.
417 R. Wilson, V. A. Lanz, C. Hueglin, Y. L. Sun, J. Tian, A. Laaksonen, T. Raatikainen, J. Rautiainen, P. Vaattovaara, M.
418 Ehn, M. Kulmala, J. M. Tomlinson, D. R. Collins, M. J. Cubison, J. Dunlea, J. A. Huffman, T. B. Onasch, M. R. Alfarra,
419 P. I. Williams, K. Bower, Y. Kondo, J. Schneider, F. Drewnick, S. Borrmann, S. Weimer, K. Demerjian, D. Salcedo, L.
420 Cottrell, R. Griffin, A. Takami, T. Miyoshi, S. Hatakeyama, A. Shimono, J. Y. Sun, Y. M. Zhang, K. Dzepina, J. R.
421 Kimmel, D. Sueper, J. T. Jayne, S. C. Herndon, A. M. Trimborn, L. R. Williams, E. C. Wood, A. M. Middlebrook, C. E.
422 Kolb, U. Baltensperger, and D. R. Worsnop : Evolution of Organic Aerosols in the Atmosphere, *Science*, 326(5959),
423 1525-1529, doi: 10.1126/science.1180353,2009.

424 Kondo, Y., H. Matsui, N. Moteki, L. Sahu, N. Takegawa, M. Kajino, Y. Zhao, M. J. Cubison, J. L. Jimenez, S. Vay, G. S.
425 Diskin, B. Anderson, A. Wisthaler, T. Mikoviny, H. E. Fuelberg, D. R. Blake, G. Huey, A. J. Weinheimer, D. J. Knapp,
426 and W. H. Brune: Emissions of black carbon, organic, and inorganic aerosols from biomass burning in North America
427 and Asia in 2008, *J. Geophys. Res.-Atmos.*, 116(D8), 353-366, doi: 10.1029/2010JD015152,2011.

428 Lanz, V. A., M. R. Alfarra, U. Baltensperger, B. Buchmann, C. Hueglin, and A. S. H. Prévôt : Source apportionment of
429 submicron organic aerosols at an urban site by factor analytical modelling of aerosol mass spectra, *Atmos. Chem. Phys.*,
430 7(6), 1503-1522, doi: 10.5194/acp-7-1503-2007,2007.

431 Lanz, V. A., A. S. H. Prévôt, M. R. Alfarra, S. Weimer, C. Mohr, P. F. DeCarlo, M. F. D. Gianini, C. Hueglin, J. Schneider,
432 O. Favez, B. D'Anna, C. George, and U. Baltensperger: Characterization of aerosol chemical composition with aerosol
433 mass spectrometry in Central Europe: an overview, *Atmos. Chem. Phys.*, 10(21), 10453-10471, doi: 10.5194/acp-10-
434 10453-2010,2010.

435 Matthew, B. M., A. M. Middlebrook, and T. B. Onasch : Collection Efficiencies in an Aerodyne Aerosol Mass Spectrometer
436 as a Function of Particle Phase for Laboratory Generated Aerosols, *Aerosol Sci. Tech.*, 42(11), 884-898, doi:
437 10.1080/02786820802356797,2008.

438 Middlebrook, A. M., R. Bahreini, J. L. Jimenez, and M. R. Canagaratna : Evaluation of Composition-Dependent Collection
439 Efficiencies for the Aerodyne Aerosol Mass Spectrometer using Field Data, *Aerosol Sci. Tech.*, 46(3), 258-271, doi:
440 10.1080/02786826.2011.620041,2012.

441 Mohr, C., P. F. DeCarlo, M. F. Heringa, R. Chirico, J. G. Slowik, R. Richter, C. Reche, A. Alastuey, X. Querol, R. Seco, J.
442 Peñuelas, J. L. Jiménez, M. Crippa, R. Zimmermann, U. Baltensperger, and A. S. H. Prévôt : Identification and

443 quantification of organic aerosol from cooking and other sources in Barcelona using aerosol mass spectrometer data,
444 *Atmos. Chem. Phys.*, 12(4), 1649-1665, doi: 10.5194/acp-12-1649-2012,2012.

445 Ng, N. L., M. R. Canagaratna, J. L. Jimenez, Q. Zhang, I. M. Ulbrich, and D. R. Worsnop : Real-Time Methods for
446 Estimating Organic Component Mass Concentrations from Aerosol Mass Spectrometer Data, *Environ. Sci. Technol.*,
447 45(3), 910-916, doi: 10.1021/es102951k,2011.

448 Paatero, P. :The Multilinear Engine: A Table-Driven, Least Squares Program for Solving Multilinear Problems, including
449 the n-Way Parallel Factor Analysis Model, *J. Comput. Graph. Stat.*, 8(4), 854-888, doi: 10.2307/1390831,1999.

450 Paatero, P., and U. Tapper : Positive matrix factorization: A non-negative factor model with optimal utilization of error
451 estimates of data values, *Environmetrics*, 5(2), 111-126, doi: 10.1002/env.3170050203,1994.

452 Pope, C. A., and D. W. Dockery : Health Effects of Fine Particulate Air Pollution: Lines that Connect, *J. Air Waste*
453 *Manage.*,56(6), 709-742, doi: 10.1080/10473289.2006.10464485,2006.

454 Pratt, K. A., and K. A. Prather : Mass spectrometry of atmospheric aerosols—Recent developments and applications. Part II:
455 On-line mass spectrometry techniques, *Mass Spectrom. Rev.*, 31(1), 17-48, doi: 10.1002/mas.20330,2012.

456 Qin, Y. M., H. B. Tan, Y. J. Li, M. I. Schurman, F. Li, F. Canonaco, A. S. H. Prévôt, and C. K. Chan : Impacts of traffic
457 emissions on atmospheric particulate nitrate and organics at a downwind site on the periphery of Guangzhou, China,
458 *Atmos. Chem. Phys.*, 17(17), 10245-10258, doi: 10.5194/acp-17-10245-2017,2017.

459 Reddy, C. M., A. Pearson, L. Xu, A. P. McNichol, B. A. Benner, S. A. Wise, G. A. Klouda, L. A. Currie, and T. I.
460 Eglinton :Radiocarbon as a Tool To Apportion the Sources of Polycyclic Aromatic Hydrocarbons and Black Carbon in
461 Environmental Samples, *Environ. Sci. Technol.*, 36(8), 1774-1782, doi: 10.1021/es011343f,2002.

462 Reyes-Villegas, E., D. C. Green, M. Priestman, F. Canonaco, H. Coe, A. S. H. Prévôt, and J. D. Allan: Organic aerosol
463 source apportionment in London 2013 with ME-2: exploring the solution space with annual and seasonal analysis,
464 *Atmos. Chem. Phys.*, 16(24), 15545-15559, doi: 10.5194/acp-16-15545-2016,2016.

465 Schmidt, M. W. I., and A. G. Noack : Black carbon in soils and sediments: Analysis, distribution, implications, and current
466 challenges, *Global Biogeochem. Cy.*, 14(3), 777-793, doi: 10.1029/1999GB001208,2000.

467 Schwarz, J. P., R. S. Gao, J. R. Spackman, L. A. Watts, D. S. Thomson, D. W. Fahey, T. B. Ryerson, J. Peischl, J. S.
468 Holloway, M. Trainer, G. J. Frost, T. Baynard, D. A. Lack, J. A. de Gouw, C. Warneke, and L. A. Del
469 Negro :Measurement of the mixing state, mass, and optical size of individual black carbon particles in urban and biomass
470 burning emissions, *Geophys. Res. Lett.*, 35(13), L13810, doi: 10.1029/2008GL033968,2008.

471 Sun, Y., W. Du, P. Fu, Q. Wang, J. Li, X. Ge, Q. Zhang, C. Zhu, L. Ren, W. Xu, J. Zhao, T. Han, D. R. Worsnop, and Z.
472 Wang : Primary and secondary aerosols in Beijing in winter: sources, variations and processes, *Atmos. Chem. Phys.*,
473 16(13), 8309-8329, doi: 10.5194/acp-16-8309-2016,2016.

474 Tian, H., Cheng, K., Wang, Y., Zhao, D., Lu, L., Jia, W. and Hao, J.: Temporal and spatial variation characteristics of
475 atmospheric emissions of Cd, Cr, and Pb from coal in China. *Atmospheric Environment*, 50: 157-163,doi:
476 10.1016/j.atmosenv.2011.12.045,2012.

477 Ulbrich, I. M., M. R. Canagaratna, Q. Zhang, D. R. Worsnop, and J. L. Jimenez : Interpretation of organic components from
478 Positive Matrix Factorization of aerosol mass spectrometric data, *Atmos. Chem. Phys.*, 9(9), 2891-2918, doi:
479 10.5194/acp-9-2891-2009,2009.

480 Wang, X., B. J. Williams, X. Wang, Y. Tang, Y. Huang, L. Kong, X. Yang, and P. Biswas : Characterization of organic
481 aerosol produced during pulverized coal combustion in a drop tube furnace, *Atmos. Chem. Phys.*, 13(21), 10919-10932,
482 doi: 10.5194/acp-13-10919-2013,2013.

483 White, H. :Black carbon in the environment, J. Wiley,1985.

484 Xu, J., Q. Zhang, M. Chen, X. Ge, J. Ren, and D. Qin: Chemical composition, sources, and processes of urban aerosols
485 during summertime in northwest China: insights from high-resolution aerosol mass spectrometry, *Atmos. Chem. Phys.*,
486 14(23), 12593-12611, doi: 10.5194/acp-14-12593-2014,2014.

487 Xu, L., S. Suresh, H. Guo, R. J. Weber, and N. L. Ng : Aerosol characterization over the southeastern United States using
488 high-resolution aerosol mass spectrometry: spatial and seasonal variation of aerosol composition and sources with a
489 focus on organic nitrates, *Atmos. Chem. Phys.*, 15(13), 7307-7336, doi: 10.5194/acp-15-7307-2015,2015.

490 Zhang, Q., J. L. Jimenez, M. R. Canagaratna, I. M. Ulbrich, N. L. Ng, D. R. Worsnop, and Y. Sun : Understanding
491 atmospheric organic aerosols via factor analysis of aerosol mass spectrometry: a review, *Anal. Bioanal. Chem.*, 401(10),
492 3045-3067, doi: 10.1007/s00216-011-5355-y,2011.

493 Zhang, Q., J. L. Jimenez, M. R. Canagaratna, J. D. Allan, H. Coe, I. Ulbrich, M. R. Alfarra, A. Takami, A. M. Middlebrook,
494 Y. L. Sun, K. Dzepina, E. Dunlea, K. Docherty, P. F. DeCarlo, D. Salcedo, T. Onasch, J. T. Jayne, T. Miyoshi, A.
495 Shimono, S. Hatakeyama, N. Takegawa, Y. Kondo, J. Schneider, F. Drewnick, S. Borrmann, S. Weimer, K. Demerjian,
496 P. Williams, K. Bower, R. Bahreini, L. Cottrell, R. J. Griffin, J. Rautiainen, J. Y. Sun, Y. M. Zhang, and D. R.
497 Worsnop :Ubiquity and dominance of oxygenated species in organic aerosols in anthropogenically-influenced Northern
498 Hemisphere midlatitudes, *Geophys. Res. Lett.*, 34(13), L13801, doi: 10.1029/2007GL029979,2007.

499 Zhang, Y., J. J. Schauer, Y. Zhang, L. Zeng, Y. Wei, Y. Liu, and M. Shao : Characteristics of Particulate Carbon Emissions
500 from Real-World Chinese Coal Combustion, *Environ Sci. Technol.*, 42(14), 5068-5073, doi: 10.1021/es7022576,2008.

501 Zhou, S., S. Collier, D. A. Jaffe, N. L. Briggs, J. Hee, A. J. Sedlacek Iii, L. Kleinman, T. B. Onasch, and Q. Zhang :
502 Regional influence of wildfires on aerosol chemistry in the western US and insights into atmospheric aging of biomass
503 burning organic aerosol, *Atmos. Chem. Phys.*, 17(3), 2477-2493, doi: 10.5194/acp-17-2477-2017,2017.

504